



Published in final edited form as:

ACS Chem Biol. 2013 April 19; 8(4): 812–822. doi:10.1021/cb300555n.

Identification of Novel Host-Targeted Compounds That Protect From Anthrax Lethal Toxin-Induced Cell Death

Louise H. Slater^{1,2,3,#}, Erik C. Hett^{1,2,3,#}, Kevin Mark^{1,2,3}, Nicole M. Chumler⁴, Deepa Patel³, D. Borden Lacy⁴, R. John Collier³, and Deborah T. Hung^{1,2,3,*}

¹Department of Molecular Biology and Center for Computational and Integrative Biology, Massachusetts General Hospital, 185 Cambridge Street, Boston, MA 02114, USA

²Infectious Disease Initiative, Broad Institute, 7 Cambridge Center, Cambridge, MA 02142, USA

³Department of Microbiology and Immunobiology, Harvard Medical School, 77 Ave Louis Pasteur Boston, MA 02115, USA

⁴Department of Microbiology and Immunology, Vanderbilt University Medical Center, A-5301 Medical Center North, 1161 21st Avenue South, Nashville, TN 37232, USA

Abstract

Studying how pathogens subvert the host to cause disease has contributed to the understanding of fundamental cell biology. *Bacillus anthracis*, the causative agent of anthrax, produces the virulence factor lethal toxin to disarm host immunity and cause pathology. We conducted a phenotypic small molecule screen to identify inhibitors of lethal toxin-induced macrophage cell death and used an ordered series of secondary assays to characterize the hits and determine their effects on cellular function. We identified a structurally diverse set of small molecules that act at various points along the lethal toxin pathway, including inhibitors of endocytosis; natural product inhibitors of organelle acidification (*e.g.* the botulinum neurotoxin inhibitor, toosendanin); and a novel proteasome inhibitor, 4MNB (4-methoxy-2-[2-(5-methoxy-2-nitrosophenyl)ethyl]-1-nitrosobenzene). Many of the compounds, including three drugs approved for use in humans, also protected against the related *Clostridium difficile* toxin TcdB, further demonstrating their value as novel tools for perturbation and study of toxin biology and host cellular processes, and highlighting potential new strategies for intervening on toxin-mediated diseases.

Introduction

Chemical perturbation of biological systems is a powerful method for studying cellular pathways and processes. Bioactive small molecules identified from forward chemical genetic screens can serve as tools to dissect these processes when linked to a target or mechanism of action. Bacterial toxins can similarly mediate such perturbations when they induce phenotypes such as cell death by co-opting or disrupting host cellular processes. Thus, the identification of small molecules that suppress toxin-induced phenotypes in chemical suppressor screens can help not only to elucidate the mechanism of intoxication and identify new therapeutic antitoxin targets, but also to provide novel tools for studying fundamental host cell biology.

*Corresponding author hung@molbio.mgh.harvard.edu.

#These authors contributed equally to this publication

Author Contributions: LHS, ECH, and DTH prepared the manuscript; LHS, ECH, KM, NMC, DP, DBL, RJC and DTH designed and conducted experiments.

Competing Financial Interests Statement: The authors have no competing interests to declare.

Anthrax toxin, which is elaborated by *Bacillus anthracis*, the causative agent of anthrax, is an example of one such toxin that co-opts a large number of host factors to enter cells and induce death. It is composed of three proteins: protective antigen (PA), lethal factor (LF) and edema factor (EF) (1). LF is a zinc metalloprotease that cleaves MAP kinase kinases (2-4) and NLRP1b (5), while EF is an adenylate cyclase (6). Individually the toxin components have no effect, but when combined in a binary fashion to form their respective AB toxins, PA and LF (forming lethal toxin, LT) cause death of experimental animals and cultured macrophages (7-10), and PA and EF (forming edema toxin, ET) cause tissue edema (11) and death in a rabbit model of inhalational anthrax (12, 13). PA, the toxin B subunit, shuttles both LF and EF into the cytosol.

After PA binds to one of two anthrax toxin receptors, it is processed by a host furin protease and oligomerizes into heptamers or octamers that relocalize to lipid rafts (14) (Fig 1). Up to three or four molecules of LF and/or EF bind to the oligomer (15, 16), and the toxin-receptor complexes undergo endocytosis. Following endocytosis, the internalized vesicles are trafficked to early endosomes, where toxin-receptor complexes are sorted into intra luminal vesicles (17). A drop in pH in the endosome causes a conformational change in PA, converting the heptamer from the prepore to the pore state, which inserts into the membrane (18-20) and forms a functional pore through which LF and EF translocate into the lumen of the intraluminal vesicles (1). LF and EF are finally delivered to the cytosol when the vesicles undergo back-fusion with the late endosomal membrane (17).

After entering the cytosol in J774A.1 cells and other susceptible murine macrophages, LT induces rapid caspase-1 dependent cell death (8). Activation of caspase-1 involves the NLRP1b inflammasome and can be prevented by proteasome inhibitors. LF has recently been shown to cleave NLRP1b from susceptible rat macrophages, although it is not clear that this signal alone is sufficient to induce caspase-1 activation and cell death (5). MAP kinase kinases are also substrates of the LF protease; however, it is currently unclear whether downregulation of the MAP kinase pathway contributes to caspase-1 dependent cell death in susceptible murine macrophages.

Previous small molecule screens for inhibitors of LT have predominantly yielded novel inhibitors of endosomal acidification, including the antiarrhythmic drugs amiodarone and bepridil (21), and known bioactive compounds diphyllin and niclosamide (22). A screen also identified the naphthoquinone NSC 95397, which has previously been described as an inhibitor of Cdc25 protein phosphatase. The exact mechanism of action of NSC 95397 was unclear, but it was proposed to protect via activation of MAP kinases to trigger an anti-apoptotic effect upon LF treatment (23).

Here, we describe an approach combining a high-throughput small molecule screen to identify novel inhibitors of host proteins involved in the LT pathway and a series of secondary assays that allow systematic elucidation of their mechanisms of action. We identified several small molecules that provide complete protection of J774A.1 murine macrophages from LT, including compounds that prevent LT internalization and a compound that prevents LT cytotoxicity by inhibiting the proteasome. Many of the identified internalization inhibitors prevented endocytosis of the toxin. Interestingly, while two natural products, the botulinum neurotoxin inhibitor toosendanin and the glycosylated sterol **5**, appear to inhibit endosome acidification, they were able to inhibit LT-induced cell death at a lower concentration than that needed to affect endosome acidification, suggesting that they may have an additional mechanism of action. However, unlike its action on botulinum neurotoxin (24), toosendanin did not appear to inhibit translocation of LF through the PA pore in *in vitro* and cell based assays. Because many toxins that need to gain access to the host cell cytosol share conserved mechanisms of entry, compounds that inhibit events

involved in toxin internalization may act as broad toxin inhibitors. We show that inhibitors of endocytosis and endosomal acidification identified in this screen, including toosendanin and three drugs approved for use in humans, also inhibit cell death induced by the bacterial toxin TcdB from *Clostridium difficile*, a pathogen of significant current interest due to the rising incidence and mortality in hospital-acquired infection.

Results and Discussion

A small molecule screen for inhibitors of anthrax LT

We performed a suppressor screen of LT by screening for compounds that rescue J774A.1 murine macrophages from LT challenge. Cells were pre-incubated with a compound library in 384 well-format for 2 hours, and then treated with PA and LF for 6 hours, which kills approximately 98% of cells. Cell survival was measured using CellTiter-Glo, a luminescence-based assay that quantitates ATP. The average Z' factor for the assay was 0.67.

A short assay time was chosen to allow us to screen inhibitors of essential cell functions that would otherwise be toxic over longer periods of time. We screened 31,350 small molecules at an average concentration of approximately 33 μ M. The libraries screened were part of the Broad Institute collection and included bioactive compounds with annotated mechanisms of action, commercially available compounds, diversity-oriented synthetic (DOS) compounds (25), natural products, and natural product extracts (Table 1). We cherry-picked the top 0.5% of compounds based on the strength of protection from LT and reproducibility between the two replicates (Table 1; Fig. 2), and re-tested them in an 8-point dose-response assay. Of these 160 compounds, 126 (79%) reproducibly rescued J774A.1 cells from death. We proceeded to follow-up with the 49 compounds that protected 100% of cells from LT and exhibited low toxicity towards J774A.1 cells in this short time-period. Active compounds identified also included the proteasome inhibitor epoxomicin, the general caspase inhibitor Boc-D-CMK, and the vacuolar ATPase inhibitor concanamycin A (26), which served as positive controls for the screen and secondary assays. Interestingly, the screen also identified three drugs approved for use in humans (pizotifen malate, disulfiram and tilorone), which could be potential therapeutics for anthrax disease (Table 2).

Secondary assays to categorize hits

We next proceeded to characterize the active compounds by performing a number of secondary assays. First, we determined whether the compounds inhibited toxin internalization (binding, uptake and delivery into the cytosol) or cytotoxicity (LF protease activity and induction of cell death). We took advantage of a toxin chimera LF_N-DTA, which is a fusion protein consisting of the N-terminal domain of LF and the enzymatic domain of diphtheria toxin. LF_N-DTA enters the cytosol in a PA-dependent manner identical to that of LF, but kills cells by a completely different mechanism involving inhibition of elongation factor 2 and activation of apoptosis. We tested the ability of compounds to protect J774A.1 cells from PA/LF_N-DTA challenge over 24 hours, as compounds that protect against both LF and LF_N-DTA likely act during internalization. In addition, the longer time course of this experiment allowed us to distinguish compounds that might exhibit toxicity to the host. Of the 46 compounds tested, we identified 15 internalization inhibitors that protected cells from both LT and PA/LF_N-DTA over 24 hours, and one cytotoxicity inhibitor (Table 2). We were unable to annotate the remaining 30 compounds due to toxicity towards J774A.1 cells over 24 hours, or because they did not protect cells from LT over this timescale. Compounds that protect cells from LT in the 6 hour assay but not the 24 hour assay, likely affect the kinetics of internalization or cytotoxicity, but do not completely block toxin action.

Next, to further confirm that compounds were internalization or cytotoxicity inhibitors, as well as to characterize the inhibitors that we were unable to assign with the 24 hour LF_N-DTA assay, we tested the ability of the compounds to protect cells against the effects of EF, which also enters in a PA-dependent manner but results in elevated cAMP levels. Using a competitive ELISA-based assay, we measured the concentration of cAMP in lysates from cells treated with ET for 5 hours. By these two assays, we identified a total of 31 LT inhibitors that prevent internalization, and 18 inhibitors of cytotoxicity (Fig. 3 and Table 2).

Multiple inhibitors of internalization prevent endocytosis

Next, to determine whether the internalization inhibitors prevent endocytosis of the toxin-receptor complex, we tested their ability to inhibit the uptake of transferrin and dextran. Iron-loaded transferrin enters cells by binding to transferrin receptors on the cell surface and undergoing clathrin-mediated endocytosis (27). Following release of Fe³⁺ in the endosome, transferrin enters the recycling endosome and is returned to the cell surface. Dextran is a hydrophilic polysaccharide that can be used as a fluid-phase marker for uptake via endocytosis, phagocytosis, or macropinocytosis (28, 29). J774A.1 cells were pre-treated with compound and then incubated with fluorescently labeled dextran and transferrin for 2 hours or 15 minutes, respectively, washed, and then fluorescence was measured using a plate reader. 23 out of 27 of the internalization inhibitors tested in this assay prevented uptake of transferrin and dextran by more than 50%, suggesting that they protect against LT by inhibiting endocytosis of the toxin (Table 2). Of note, we found that the naphthoquinone NSC 95397 (compound 4), is an internalization inhibitor that prevents transferrin and dextran uptake. NSC 95397 has previously been identified in a small molecule screen of LT inhibitors and was suggested to protect against LT induced cell death by inhibiting MEK cleavage, as well as to upregulate MAP kinase signaling (23). Here, we show that, in fact, NSC 95397 protects against LT induced cell death by inhibiting toxin uptake.

The enrichment for endocytosis inhibitors could be due to the complexity of endocytosis and its requirement for numerous host proteins, such as actin, clathrin, and the unconventional adaptor AP-1 (30, 31). Furthermore, endocytosis of toxin-receptor complexes is regulated by post-translational modifications of anthrax toxin receptors. In the absence of PA binding, toxin receptors are palmitoylated (32), which serves to prevent endocytosis and receptor turnover in the absence of ligand. PA binding triggers redistribution of the PA-receptor complexes to cholesterol-rich lipid rafts (30), likely due to a conformational change in the receptor that causes depalmitoylation or association with other membrane proteins. Src-kinase mediated tyrosine phosphorylation of the cytoplasmic tail of the receptors recruits the E3 ligase Cbl in a β -arrestin-dependent manner (31, 33), leading to ubiquitination of the cytoplasmic tail and thus promoting interaction with components of the endocytic machinery that contain Ub-interacting domains.

Toosendanin inhibits entry of LT into the cytoplasm

Three of the internalization inhibitors are natural products, or natural product extracts, that did not inhibit uptake of dextran and transferrin (Table 2). Two of the natural products (extracts 31 and 32) were fractions of an extract from the plant *Melia azedarach*, while the structure of the third natural product, the glycosylated sterol 5 (IC₅₀ 1.25 μ M), was known (Fig. 3). Extract 32 was particularly potent, with an upper IC₅₀ limit of 10 ng ml⁻¹, assuming that the extract consisted only of the active molecule.

Because 31 and 32 are both from *Melia azedarach*, we searched for known compounds produced by this plant. Toosendanin is a triterpenoid from *Melia azedarach*(34), and has been described to have *in vivo* activity against botulinum neurotoxin (BoNT) (24, 35-37) (Fig. 3). We found that toosendanin phenocopied the effects of 31 and 32, by preventing LT

and PA/LF_N-DTA-induced cell death without inhibiting transferrin and dextran uptake. Toosendanin had an IC₅₀ of 56 nM (32 ng ml⁻¹) against LT, indicating that it is likely the active compound in these extracts (Fig. 4).

Since pore formation and translocation of LF require an acidic endosome, we tested whether toosendanin and sterol **5** inhibit organelle acidification using the cell-permeable pH-sensitive dye lysotracker red, which accumulates in acidic organelles. Cells were preincubated with compound, and then incubated with lysotracker red, before measuring fluorescence using a plate reader. Since lysotracker staining responds to changes in pH in both endosomes (pH 5–6.5) and lysosomes (pH 4–5), full inhibition of lysotracker staining suggests that both endosomes and lysosomes are neutralized, while partial inhibition of lysotracker staining likely corresponds to neutralization of endosomes but not lysosomes. Therefore, as noted for the vacuolar ATPase inhibitor concanamycin A (Figure 4, 25 nM) full inhibition from LT-induced cell death corresponds to around 60% inhibition of lysotracker staining.

We found that both toosendanin and **5**, along with concanamycin A, inhibited lysotracker staining at sufficiently high concentrations (Fig. 4). However, we noted that in contrast to the positive control concanamycin A, toosendanin and **5** protect close to 100% of cells from LT at concentrations where they exhibit minimal or no inhibition of lysotracker staining (Fig. 4). For example, 5 μM **5** protected 84% of cells from LT, but had no effect on lysotracker staining, while 183 nM toosendanin protected 92% of cells from LT but inhibited only 23% of lysotracker staining (Fig. 4). These results raise the possibility that while these compounds do inhibit endosomal acidification at higher concentrations, at lower concentrations where protection against LT is still observed they may inhibit internalization by a different mechanism.

Toosendanin has been reported to protect cells against botulinum toxin (BoNT), produced by the pathogen *Clostridium botulinum*. BoNT is an AB toxin that enters cells via the endocytic route in a similar manner to LT. Previously, toosendanin has been shown to inhibit BoNT oligomerization and channel formation by the heavy chain (38, 39), and to directly inhibit light chain translocation by stabilizing the interaction between the light and heavy chains (24). Given the similarities between anthrax toxin and BoNT translocation, we hypothesized that toosendanin could inhibit LT by a similar mechanism. However, toosendanin appeared to have no effect on LF_N translocation through PA pores formed in planar lipid bilayers, or on LT-induced cell death when PA pore formation in the plasma membrane and LF translocation into the cytoplasm was initiated by a low pH pulse (data not shown). This suggests that toosendanin may protect cells from LT and BoNT by different mechanisms.

Toosendanin appears to be a potent inhibitor of LT-induced cell death, and our data suggest that it may protect cells via more than one mechanism. Toosendanin is known to have inhibitory and excitatory effects on a broad range of membrane ion channels, including potassium channels, calcium channels, and the botulinum neurotoxin (BoNT) channel, and therefore disruption of the vacuolar ATPase could explain its inhibition of endosomal acidification (24, 40-45). Interestingly, toosendanin has inhibitory activity against BoNT in animal models (24, 35-37), and has also been shown to inhibit hepatitis C virus replication in a cell culture model (46), suggesting that it might be a useful therapeutic agent in a variety of infectious diseases, including anthrax.

Inhibitors of toxin entry also protect against the AB toxin TcdB

We hypothesized that compounds that inhibit LT, ET and PA/LF_N-DTA might also inhibit related AB toxins, given the conservation of some mechanisms in the uptake of several

different toxins, such as endocytosis and endosomal acidification. Thus, we sought to test the identified internalization inhibitors against the toxin TcdB from *Clostridium difficile*. TcdB is an AB toxin that enters the cytosol through a self-made pore in the endosomal membrane in a similar manner to LT. Once in the cytosol, TcdB glycosylates the small GTPases Rho, Rac and Cdc42, causing actin depolymerization and ultimately cell death (47, 48). Almost all of the internalization inhibitors that prevented transferrin and dextran, as well as toosendanin and the endosomal acidification inhibitor **5**, also protected J774A.1 cells from TcdB (Table 2). Notably, the approved drugs piztofen malate, tilorone and disulfiram were among the inhibitors of TcdB, further demonstrating the value of these novel compounds as potential therapeutics, and as tools to study toxin and host cell biology. Of note, toosendanin protected only 30% of cells from TcdB, while the endosomal acidification inhibitor concanamycin A afforded 100% protection. This suggests that toosendanin does not strongly inhibit endosome acidification, supporting the hypothesis that it likely provides 100% protection from LT by an additional mechanism.

4MNB is a novel cytotoxicity inhibitor

One small molecule of interest that was identified as a cytotoxicity inhibitor is the compound 4-methoxy-2-[2-(5-methoxy-2-nitrosophenyl)ethyl]-1-nitrosobenzene (4MNB, Fig. 5a), which completely protects J774A.1 macrophages from LT-induced death at 40 μ M and has an IC₅₀ of ~18 μ M (Fig. 5b). Washing cells after treatment with 4MNB (or Boc-D-CMK (49)) does not dramatically reduce the protection of macrophages from LT at several concentrations of 4MNB (Fig. 5c), suggesting it is an irreversible inhibitor. 4MNB did not inhibit the increase in cAMP concentration induced by ET, indicating that it acts after toxin internalization (Fig 5d).

4MNB does not protect from LT by inhibition of Bcl-2/Bcl-XL

4MNB was previously reported to bind and inhibit Bcl-2 and Bcl-XL (50, 51), which are homologous anti-apoptotic factors that protect cells from death by binding to Apaf-1 and preventing activation of caspase-9 (52, 53). To test if inhibition of Bcl-2/Bcl-XL could account for 4MNB's observed inhibition of LT cytotoxicity, we tested several well-known inhibitors of Bcl-2/Bcl-XL including HA14-1, 2-methoxy-antimycin A3, Gossypol, and Antimycin A (54). None of these inhibitors protected cells from LT-induced cell death at any of the concentrations tested (data not shown), indicating that 4MNB protects from LT-induced cytotoxicity via a different target.

4MNB does not affect MEK cleavage

Because LF is a metalloprotease that cleaves the cytosolic MEK signaling molecules (2), we tested whether 4MNB inhibits the protease activity of LF. We treated macrophages with 4MNB prior to LT exposure, then harvested lysate and probed by Western blot analysis for evidence of MEK3 cleavage. While the internalization inhibitor concanamycin A prevents MEK cleavage by preventing translocation of LF into the cytosol, 4MNB did not prevent MEK3 cleavage at concentrations that protect cells from LT-induced death (Fig. 5e). These data confirm that 4MNB does not affect translocation of LF into the cytosol and demonstrate that it does not inhibit the protease activity of LF in whole cells.

4MNB is a novel proteasome inhibitor

We next examined whether 4MNB protects cells from LT by inhibiting the protease activity of the proteasome. If 4MNB directly inhibits the proteasome, it should affect one of three protease activities of the proteasome: chymotrypsin-like, trypsin-like, or caspase-like activity. To test this possibility, we treated macrophage lysate with 4MNB, or a known proteasome inhibitor control, epoxomicin (Epoxo) (55), and then added one of three

synthetic proteasome substrates that result in fluorescence when cleaved by the corresponding specific protease activity. Using this assay, we found that 4MNB directly inhibits all three proteasome protease activities *in vitro* (Fig. 5f).

To further confirm these results, we assayed the activity of three proteasomal protease activities in intact cells, in the presence and absence of 4MNB. We used three different cell permeable substrates specific for each protease activity that result in luminescence upon cleavage and tested for protection from LT-induced death in a parallel assay. 4MNB inhibits the proteasome trypsin and chymotrypsin-like protease activities at concentrations close to that required for protection of macrophages from LT, but not the caspase-like activity (Fig. 5g). These data demonstrate that in addition to the previously reported inhibition of Bcl-2/Bcl-XL, 4MNB also directly inhibits two of the protease activities of the proteasome *in vivo*.

To demonstrate that 4MNB can prevent the degradation of true cellular proteasome substrates, we tested its ability to inhibit the canonical LPS (lipopolysaccharide)-induced I κ B β degradation that results in NF κ B activation. Cells were treated with 4MNB followed by LPS for different time-periods to stimulate the degradation of I κ B β . Lysates were then harvested and assayed by Western blot analysis for the presence of I κ B β . In untreated (DMSO) cells, a dramatic reduction in I κ B β occurs by 40 minutes; however, 4MNB prevents the degradation of I κ B β similar to the control proteasome inhibitor Mg132 (Fig. 5h). These data demonstrate that 4MNB protects macrophages from LT-induced death through inhibition of the protease activity of the proteasome.

In summary, 4MNB did not inhibit the increase in cAMP concentration induced by ET or cleavage of MEK3 by LF in intact cells, but did inhibit proteasome protease activity *in vitro* and *in vivo*. Despite its ability to inhibit all three protease activities *in vitro*, 4MNB appears to only inhibit the trypsin and chymotrypsin-like activities to a significant degree *in vivo*, leaving the caspase-like activity intact in treated cells. 4MNB also inhibited I κ B β degradation, indicating that its activity extends beyond substrates in the LT pathway.

Conclusion

Through a forward chemical genetic screen, we have identified several novel small molecule inhibitors of LT-induced cell death, including three drugs approved for use in humans that could potentially be used as anti-toxin therapeutics. We screened a diverse set of small molecules, and note that the top hits were enriched for bioactive small molecules and natural products (Table 1). We characterized hits from the screen by performing an ordered series of secondary assays based on current knowledge of the LT pathway to elucidate their function – assessing whether the compounds were internalization inhibitors (compounds that prevent cytosolic delivery of toxin), or cytotoxicity inhibitors (compounds that inhibit cytotoxicity induced by LF protease activity in the cytosol). We found that a large proportion of the hits were inhibitors of internalization, which is not surprising, given the large number of host proteins and numerous steps involved in toxin trafficking (e.g. delivery of toxin from the endosome to the cytosol, sorting of the toxin-receptor complexes into intraluminal vesicles, PA pore formation, translocation of LF and EF into the lumen of the intraluminal vesicle, and back-fusion of the vesicles with the late endosomal membrane to deliver toxin into the cytosol (17)). We also identified a number of compounds that inhibited cytotoxicity. Of particular interest, we found that 4MNB is a novel proteasome inhibitor that does not affect toxin entry.

Since the steps involved in internalization are required for many essential cellular processes, it is possible that inhibitors of these processes could exhibit toxicity to the host cell or

organism. Indeed, we found that 8 compounds were toxic to J774A.1 macrophages over 24 hours (Table 2), which could preclude their use in *in vivo* assays. However, these compounds remain useful tools for studying the LT pathway and host cell biology.

The identification of novel host-targeted inhibitors of LT-induced cell death provides a structurally diverse set of tool compounds that can be used to perturb and study both the LT pathway and fundamental cellular processes. By systematically applying a series of secondary assays, we were able to assign mechanisms of action to inhibitors. In some cases such as too send an in and NSC 95397, the inhibitors appear to have multiple possible mechanisms by which they protect against LT. However, with further investigation, these mechanisms can be distinguished to clarify the relevant mode of action to LT intoxication.

Methods

Cells, antibodies and reagents

J774A.1 cells were obtained from American Type Cell Culture Collection (ATCC) and cultured in Dulbecco's Modified Eagle Medium (DMEM) (Gibco) containing L-glutamine, 10% (v/v) fetal bovine serum (Hyclone) and penicillin-streptomycin (Mediatech Inc.), and maintained at 37 °C with a humidified atmosphere containing 5% CO₂. Secondary HRP goat anti-rabbit antibody, and antibodies to MEK3 (sc-959), I κ B β (sc-9130), and actin were from Santz Cruz Biotechnology. LF_NDTA (56) was a kind gift from the Collier lab (Harvard Medical School). EF was obtained from List Biological Laboratories. Compounds were obtained from Spectrum Chemicals, Gaia Chemical Corporation, Ryan Life Sciences, Biomol International, Alexis Biochemicals Calbiochem, and EMD. LF substrate 3 was from Calbiochem, and proteasome substrates from Promega.

Protein expression and purification

PA and LF were expressed in BL21STAR(DE3) *Escherichia coli* grown in ECPM1 medium (57). Cultures were induced at 30°C with isopropyl-1-thio- β -D-galactopyranoside (IPTG).

Recombinant PA was overexpressed in the periplasm from pET22b (Invitrogen). Periplasmic proteins were purified by osmotic shock by first resuspending pelleted cells in 4 mL of 20% (v/v) sucrose, 1 mM EDTA, and 20 mM Tris-HCl (pH 8.5) per gram of cells. Cells were then resuspended in 5 mM magnesium sulfate with 20 mM Tris-HCl pH 8.5 and 1 mM PMSF, and the periplasmic fraction clarified by centrifugation. PA was purified by anion-exchange chromatography followed by size-exclusion chromatography using an S-200 Superdex gel filtration column (Amersham Biosciences) (58).

His₆-tagged LF cloned into pET15b was purified as previously described (56, 59). Cells were resuspended in 50 mM Tris-HCl pH 7.5, 150 mM sodium chloride with 1 \times Complete Protease Inhibitor without EDTA, lysozyme and DNase I, then sonicated and centrifuged to clarify the lysate. His₆-tagged protein was purified by nickel column, and the N-terminal H6-tag removed by thrombin cleavage overnight at 25°C in Buffer C with 2.5 mM calcium chloride and 2.1 U thrombin mg⁻¹ protein (GE Healthcare). Proteins were further purified by anion exchange and size exclusion chromatography as described above.

TcdB was purified from *C. difficile* strain VPI 10463 according to published methods. Protein purity was assessed by SDS-PAGE (60).

High-throughput small molecule screen

4 \times 10 J774A.1 cells in 20 μ L were plated in white 384-well plates and incubated overnight. 100 nL of compound in DMSO was transferred to plates, and cells were incubated for 2

hours at 37 °C. 10 μ L of LT (16 nM PA, 8 nM LF) was added, and cells were incubated at 37 °C for 6 hours. Cell viability was assessed by adding an equal volume of Cell Titer Glo diluted 1:6 in PBS and measuring luminescence using an Envision Multilabel Plate reader. Compounds were screened in duplicate, and raw data was submitted to the Broad Chemical Biology screening platform for data analysis and calculation of z scores. ($z = (x - \mu)/\sigma$ where x is the raw luminescence score, μ is the mean of the mock- (DMSO) treated well, and σ is the standard deviation of the mock-treated wells.)

Small molecule retesting and PA/LF_N-DTA assay

Compounds were retested in duplicate with 8-point dose response curves, with typical concentrations between 33 μ M and 0.015 μ M in 3-fold dilutions. LT (16 nM PA, 8 nM LF) was added and cells were incubated at 37 °C for 6 hours. Cells were also screened with LT (16 nM PA, 660 pM LF) for 24 hours, with PA/LF_NDTA (16 nM PA, 100 pM LF_NDTA) for 24 hours, and with compound alone for 24 hours to assess toxicity. Cell Titer Glo was used to measure cell viability as described previously.

ET assay

5×10^4 J774A.1 cells in 100 μ L were plated in 96-well plates, and incubated overnight. Cells were preincubated with compound for 2 hours, before the addition of ET (11 nM PA, 1.2 nM EF) for 5 hours at 37 °C. The concentration of cAMP in cell lysates was measured by cAMP enzyme immunoassay according to the manufacturers instructions (Enzo Life Sciences).

Transferrin/dextran

3.5×10^4 J774A.1 cells were plated in black, optical 96-well plates and incubated overnight. Cells were pretreated with compound for 2 hours, followed by addition of dextran-Alexa Fluor 488 10,000 MW (100 μ g ml⁻¹) (Invitrogen) and incubation at 37 °C for 75 minutes, and then addition of transferrin-Alexa Fluor 546 (10 μ g ml⁻¹) (Invitrogen) and incubation at 37 °C for 15 minutes. Cells were washed with $3 \times 100 \mu$ L DMEM (without phenol red), and 50 μ L PBS was added to plates. Fluorescence was measured using a SpectraMax M5 plate reader (Molecular Devices) to assess transferrin and dextran uptake. Cell Titer Glo was added to the plate to measure the number of cells in each well.

TcdB assay

9×10^4 Chinese Hamster Ovary (CHO) cells in 30 μ L were plated in white 384 well plates containing compound and incubated at 37 °C for 2 hours. TcdB (35 nM) was added and the cells were incubated at 37 °C for 3 hours. CellTiterGlo was used to measure cell viability as previously described.

Lysotracker assay

3.5×10^4 J774A.1 cells were plated in black, optical 96-well plates and incubated overnight. Cells were pretreated with compound for 2 hours, followed by addition of lysotracker red DND-99 (100 nM) (Invitrogen) and incubation for 1 hour at 37 °C. Cells were washed with $3 \times 100 \mu$ L DMEM (without phenol red), and fixed with 4% (w/v) paraformaldehyde. Fluorescence was measured using a SpectraMax M5 plate reader.

MEK cleavage assay

1×10^6 macrophages were plated per well in a 6-well dish overnight. Cells were incubated with compound for 2 hours, then LT (LF 1-2 nM and PA 11 nM) was added and cells were incubated for 2 hours. Total cell lysates were made, protein concentrations were measured

and normalized, and proteins were separated on an SDS-PAGE, transferred to PVDF, and probed with anti-MEK3 antibodies.

Whole cell proteasome assay

5×10^5 macrophages per well were plated in a 96-well plate and incubated overnight. Cells were then preincubated with compound for 2 hours and then mixed with cell-permeable substrates in the provided buffer (Promega). Kinetic reads of luminescence were taken every 5 minutes for 30 minutes.

In vitro proteasome assay

7×10^6 cells were plated in 10cm dishes, incubated overnight, washed with PBS, and harvested in assay buffer (50 mM Tris [pH 7.5], 140 mM NaCl, 5 mM $MgCl_2$, 1 mM EGTA, 10% (v/v) glycerol, 0.5 mM DTT, 2 mM ATP, and protease inhibitor cocktail (Sigma)). Cells were lysed using sonication, and lysate was diluted in assay buffer and distributed into wells of a 384 or 96-well plate. Compound was added, then substrate (ProteasomeGlo, Promega) was added quickly and kinetic readings were taken for fluorescence or luminescence (depending on substrate used).

I κ B β blot

Cells were treated in 6-well plates with compounds for 2 hours, then treated with 100 ng ml^{-1} LPS for the indicated period of time. Lysates were probed by Western blot for I κ B β and actin for loading control. In a parallel LT assay, all compounds protected ~100% from LT-induced cell death.

Acknowledgments

We would like to thank A. Barker for help with production and purification of PA and LF; A. Clatworthy and S. Chiang for helpful discussions; and the Broad Institute chemical screening platform for technical help. ECH was funded by an NIH National Research Service Award fellowship F32AI084323. This work was supported in part by NIH U54 AI057159 to the New England Center of Excellence/Biodefense and Emerging Infectious Diseases (DTH).

References

1. Collier RJ. Membrane translocation by anthrax toxin. *Mol Aspects Med.* 2009; 30:413–422. [PubMed: 19563824]
2. Duesbery NS, Webb CP, Leppla SH, Gordon VM, Klimpel KR, Copeland TD, Ahn NG, Oskarsson MK, Fukasawa K, Paull KD, Vande Woude GF. Proteolytic inactivation of MAP-kinase-kinase by anthrax lethal factor. *Science.* 1998; 280:734–737. [PubMed: 9563949]
3. Vitale G, Bernardi L, Napolitani G, Mock M, Montecucco C. Susceptibility of mitogen-activated protein kinase kinase family members to proteolysis by anthrax lethal factor. *Biochem J.* 2000; 352 Pt 3:739–745. [PubMed: 11104681]
4. Vitale G, Pellizzari R, Recchi C, Napolitani G, Mock M, Montecucco C. Anthrax lethal factor cleaves the N-terminus of MAPKKs and induces tyrosine/threonine phosphorylation of MAPKs in cultured macrophages. *Biochem Biophys Res Commun.* 1998; 248:706–711. [PubMed: 9703991]
5. Levinsohn JL, Newman ZL, Hellmich KA, Fattah R, Getz MA, Liu S, Sastalla I, Leppla SH, Moayeri M. Anthrax lethal factor cleavage of nlrp1 is required for activation of the inflammasome. *PLoS Pathog.* 2012; 8:e1002638. [PubMed: 22479187]
6. Leppla SH. Anthrax toxin edema factor: a bacterial adenylate cyclase that increases cyclic AMP concentrations of eukaryotic cells. *Proc Natl Acad Sci U S A.* 1982; 79:3162–3166. [PubMed: 6285339]
7. Boyden ED, Dietrich WF. Nalp1b controls mouse macrophage susceptibility to anthrax lethal toxin. *Nat Genet.* 2006; 38:240–244. [PubMed: 16429160]

8. Fink SL, Bergsbaken T, Cookson BT. Anthrax lethal toxin and Salmonella elicit the common cell death pathway of caspase-1-dependent pyroptosis via distinct mechanisms. *Proc Natl Acad Sci U S A*. 2008; 105:4312–4317. [PubMed: 18337499]
9. Muehlbauer SM, Evering TH, Bonuccelli G, Squires RC, Ashton AW, Porcelli SA, Lisanti MP, Brojatsch J. Anthrax lethal toxin kills macrophages in a strain-specific manner by apoptosis or caspase-1-mediated necrosis. *Cell Cycle*. 2007; 6:758–766. [PubMed: 17374996]
10. Welkos SL, Keener TJ, Gibbs PH. Differences in susceptibility of inbred mice to *Bacillus anthracis*. *Infect Immun*. 1986; 51:795–800. [PubMed: 3081444]
11. Stanley JL, Smith H. Purification of factor I and recognition of a third factor of the anthrax toxin. *J Gen Microbiol*. 1961; 26:49–63. [PubMed: 13916257]
12. Levy H, Weiss S, Altboum Z, Schlomovitz J, Rothschild N, Glinert I, Sittner A, Kobiler D. The effect of deletion of the edema factor on *Bacillus anthracis* pathogenicity in guinea pigs and rabbits. *Microb Pathog*. 2012; 52:55–60. [PubMed: 22020310]
13. Lovchik JA, Drysdale M, Koehler TM, Hutt JA, Lyons CR. Expression of either lethal toxin or edema toxin by *Bacillus anthracis* is sufficient for virulence in a rabbit model of inhalational anthrax. *Infect Immun*. 2012; 80:2414–2425. [PubMed: 22526673]
14. van der Goot G, Young JA. Receptors of anthrax toxin and cell entry. *Mol Aspects Med*. 2009; 30:406–412. [PubMed: 19732789]
15. Feld GK, Thoren KL, Kintzer AF, Sterling HJ, Tang II, Greenberg SG, Williams ER, Krantz BA. Structural basis for the unfolding of anthrax lethal factor by protective antigen oligomers. *Nat Struct Mol Biol*. 2010; 17:1383–1390. [PubMed: 21037566]
16. Mogridge J, Cunningham K, Collier RJ. Stoichiometry of anthrax toxin complexes. *Biochemistry*. 2002; 41:1079–1082. [PubMed: 11790132]
17. Abrami L, Lindsay M, Parton RG, Leppla SH, van der Goot FG. Membrane insertion of anthrax protective antigen and cytoplasmic delivery of lethal factor occur at different stages of the endocytic pathway. *J Cell Biol*. 2004; 166:645–651. [PubMed: 15337774]
18. Friedlander AM. Macrophages are sensitive to anthrax lethal toxin through an acid-dependent process. *J Biol Chem*. 1986; 261:7123–7126. [PubMed: 3711080]
19. Milne JC, Furlong D, Hanna PC, Wall JS, Collier RJ. Anthrax protective antigen forms oligomers during intoxication of mammalian cells. *J Biol Chem*. 1994; 269:20607–20612. [PubMed: 8051159]
20. Milne JC, Collier RJ. pH-dependent permeabilization of the plasma membrane of mammalian cells by anthrax protective antigen. *Mol Microbiol*. 1993; 10:647–653. [PubMed: 7968541]
21. Sanchez AM, Thomas D, Gillespie EJ, Damoiseaux R, Rogers J, Saxe JP, Huang J, Manchester M, Bradley KA. Amiodarone and bepridil inhibit anthrax toxin entry into host cells. *Antimicrob Agents Chemother*. 2007; 51:2403–2411. [PubMed: 17485504]
22. Zhu PJ, Hobson JP, Southall N, Qiu C, Thomas CJ, Lu J, Inglese J, Zheng W, Leppla SH, Bugge TH, Austin CP, Liu S. Quantitative high-throughput screening identifies inhibitors of anthrax-induced cell death. *Bioorg Med Chem*. 2009; 17:5139–5145. [PubMed: 19540764]
23. Panchal RG, Ruthel G, Brittingham KC, Lane D, Kenny TA, Gussio R, Lazo JS, Bavari S. Chemical genetic screening identifies critical pathways in anthrax lethal toxin-induced pathogenesis. *Chem Biol*. 2007; 14:245–255. [PubMed: 17379140]
24. Fischer A, Nakai Y, Eubanks LM, Clancy CM, Tepp WH, Pellett S, Dickerson TJ, Johnson EA, Janda KD, Montal M. Bimodal modulation of the botulinum neurotoxin protein-conducting channel. *Proc Natl Acad Sci U S A*. 2009; 106:1330–1335. [PubMed: 19164566]
25. Burke MD, Berger EM, Schreiber SL. A synthesis strategy yielding skeletally diverse small molecules combinatorially. *J Am Chem Soc*. 2004; 126:14095–14104. [PubMed: 15506774]
26. Drose S, Bindseil KU, Bowman EJ, Siebers A, Zeeck A, Altendorf K. Inhibitory effect of modified bafilomycins and concanamycins on P- and V-type adenosinetriphosphatases. *Biochemistry*. 1993; 32:3902–3906. [PubMed: 8385991]
27. Mayle KM, Le AM, Kamei DT. The intracellular trafficking pathway of transferrin. *Biochim Biophys Acta*. 2011
28. Geisow MJ, Evans WH. pH in the endosome. Measurements during pinocytosis and receptor-mediated endocytosis. *Exp Cell Res*. 1984; 150:36–46. [PubMed: 6198190]

29. Murphy RF. Analysis and isolation of endocytic vesicles by flow cytometry and sorting: demonstration of three kinetically distinct compartments involved in fluid-phase endocytosis. *Proc Natl Acad Sci U S A*. 1985; 82:8523–8526. [PubMed: 2867544]
30. Abrami L, Liu S, Cosson P, Leppla SH, van der Goot FG. Anthrax toxin triggers endocytosis of its receptor via a lipid raft-mediated clathrin-dependent process. *J Cell Biol*. 2003; 160:321–328. [PubMed: 12551953]
31. Abrami L, Bischofberger M, Kunz B, Groux R, van der Goot FG. Endocytosis of the anthrax toxin is mediated by clathrin, actin and unconventional adaptors. *PLoS Pathog*. 2010; 6:e1000792. [PubMed: 20221438]
32. Abrami L, Leppla SH, van der Goot FG. Receptor palmitoylation and ubiquitination regulate anthrax toxin endocytosis. *J Cell Biol*. 2006; 172:309–320. [PubMed: 16401723]
33. Abrami L, Kunz B, van der Goot FG. Anthrax toxin triggers the activation of src-like kinases to mediate its own uptake. *Proc Natl Acad Sci U S A*. 2010; 107:1420–1424. [PubMed: 20080640]
34. Wang Wen-Lu WY, Chiu Shin-F N. The toxic chemical factors in the fruits of *Melia azedarach* and their bio-activities towards *Pieris rapae*. *Acta Entomologica Sinica*. 1994; 37:20–24.
35. Shih YL, Hsu K. Anti-botulismic effect of toosendanin and its facilitatory action on miniature end-plate potentials. *Jpn J Physiol*. 1983; 33:677–680. [PubMed: 6315997]
36. Zou J, Miao WY, Ding FH, Meng JY, Ye HJ, Jia GR, He XY, Sun GZ, Li PZ. The effect of toosendanin on monkey botulism. *J Tradit Chin Med*. 1985; 5:29–30. [PubMed: 3849628]
37. Zhou JY, Wang ZF, Ren XM, Tang MZ, Shi YL. Antagonism of botulinum toxin type A-induced cleavage of SNAP-25 in rat cerebral synaptosome by toosendanin. *FEBS Lett*. 2003; 555:375–379. [PubMed: 14644446]
38. Li MF, Shi YL. Toosendanin interferes with pore formation of botulinum toxin type A in PC12 cell membrane. *Acta Pharmacol Sin*. 2006; 27:66–70. [PubMed: 16364212]
39. Sun S, Suresh S, Liu H, Tepp WH, Johnson EA, Edwardson JM, Chapman ER. Receptor binding enables botulinum neurotoxin B to sense low pH for translocation channel assembly. *Cell Host Microbe*. 2011; 10:237–247. [PubMed: 21925111]
40. Shi YL, Li MF. Biological effects of toosendanin, a triterpenoid extracted from Chinese traditional medicine. *Prog Neurobiol*. 2007; 82:1–10. [PubMed: 17363132]
41. Wang ZF, Shi YL. Modulation of inward rectifier potassium channel by toosendanin, a presynaptic blocker. *Neurosci Res*. 2001; 40:211–215. [PubMed: 11448512]
42. Wang ZF, Shi YL. Inhibition of large-conductance Ca(2+)-activated K(+) channels in hippocampal neurons by toosendanin. *Neuroscience*. 2001; 104:41–47. [PubMed: 11311529]
43. Wang ZF, Shi YL. Toosendanin-induced inhibition of small-conductance calcium-activated potassium channels in CA1 pyramidal neurons of rat hippocampus. *Neurosci Lett*. 2001; 303:13–16. [PubMed: 11297812]
44. Li MF, Shi YL. Toosendanin, a triterpenoid derivative, acts as a novel agonist of L-type Ca²⁺ channels in neonatal rat ventricular cells. *Eur J Pharmacol*. 2004; 501:71–78. [PubMed: 15464064]
45. Li MF, Wu Y, Wang ZF, Shi YL. Toosendanin, a triterpenoid derivative, increases Ca²⁺ current in NG108-15 cells via L-type channels. *Neurosci Res*. 2004; 49:197–203. [PubMed: 15140562]
46. Watanabe T, Sakamoto N, Nakagawa M, Kakinuma S, Itsui Y, Nishimura-Sakurai Y, Ueyama M, Funaoka Y, Kitazume A, Nitta S, Kiyohashi K, Murakawa M, Azuma S, Tsuchiya K, Oooka S, Watanabe M. Inhibitory effect of a triterpenoid compound, with or without alpha interferon, on hepatitis C virus infection. *Antimicrob Agents Chemother*. 2011; 55:2537–2545. [PubMed: 21444704]
47. Voth DE, Ballard JD. *Clostridium difficile* toxins: mechanism of action and role in disease. *Clin Microbiol Rev*. 2005; 18:247–263. [PubMed: 15831824]
48. Papatheodorou P, Zamboglou C, Genisyuerk S, Guttenberg G, Aktories K. Clostridial glucosylating toxins enter cells via clathrin-mediated endocytosis. *PLoS One*. 2010; 5:e10673. [PubMed: 20498856]
49. Squires RC, Muehlbauer SM, Brojatsch J. Proteasomes control caspase-1 activation in anthrax lethal toxin-mediated cell killing. *J Biol Chem*. 2007; 282:34260–34267. [PubMed: 17878154]
50. Zheng CH, Zhou YJ, Zhu J, Ji HT, Chen J, Li YW, Sheng CQ, Lu JG, Jiang JH, Tang H, Song YL. Construction of a three-dimensional pharmacophore for Bcl-2 inhibitors by flexible docking and

the multiple copy simultaneous search method. *Bioorg Med Chem.* 2007; 15:6407–6417. [PubMed: 17629704]

51. Enyedy IJ, Ling Y, Nacro K, Tomita Y, Wu X, Cao Y, Guo R, Li B, Zhu X, Huang Y, Long YQ, Roller PP, Yang D, Wang S. Discovery of small-molecule inhibitors of Bcl-2 through structure-based computer screening. *J Med Chem.* 2001; 44:4313–4324. [PubMed: 11728179]
52. Huang DC, Adams JM, Cory S. The conserved N-terminal BH4 domain of Bcl-2 homologues is essential for inhibition of apoptosis and interaction with CED-4. *Embo J.* 1998; 17:1029–1039. [PubMed: 9463381]
53. Pan G, O'Rourke K, Dixit VM. Caspase-9, Bcl-XL, and Apaf-1 form a ternary complex. *J Biol Chem.* 1998; 273:5841–5845. [PubMed: 9488720]
54. Vogler M, Dinsdale D, Dyer MJ, Cohen GM. Bcl-2 inhibitors: small molecules with a big impact on cancer therapy. *Cell Death Differ.* 2009; 16:360–367. [PubMed: 18806758]
55. Meng L, Mohan R, Kwok BH, Eloffson M, Sin N, Crews CM. Epoxomicin, a potent and selective proteasome inhibitor, exhibits in vivo antiinflammatory activity. *Proc Natl Acad Sci U S A.* 1999; 96:10403–10408. [PubMed: 10468620]
56. Milne JC, Blanke SR, Hanna PC, Collier RJ. Protective antigen-binding domain of anthrax lethal factor mediates translocation of a heterologous protein fused to its amino- or carboxy-terminus. *Mol Microbiol.* 1995; 15:661–666. [PubMed: 7783638]
57. Bernard A, Payton M. Fermentation and growth of *Escherichia coli* for optimal protein production. *Curr Protoc Protein Sci.* 2001; Chapter 5 Unit5 3.
58. Miller CJ, Elliott JL, Collier RJ. Anthrax protective antigen: prepore-to-pore conversion. *Biochemistry.* 1999; 38:10432–10441. [PubMed: 10441138]
59. Zhang S, Finkelstein A, Collier RJ. Evidence that translocation of anthrax toxin's lethal factor is initiated by entry of its N terminus into the protective antigen channel. *Proc Natl Acad Sci U S A.* 2004; 101:16756–16761. [PubMed: 15548616]
60. Qa'Dan M, Spyres LM, Ballard JD. pH-induced conformational changes in *Clostridium difficile* toxin B. *Infect Immun.* 2000; 68:2470–2474. [PubMed: 10768933]
61. Muroi M, Shiragami N, Takatsuki A. Destruxin B, a specific and readily reversible inhibitor of vacuolar-type H(+)-translocating ATPase. *Biochem Biophys Res Commun.* 1994; 205:1358–1365. [PubMed: 7802670]
62. Lyss G, Knorre A, Schmidt TJ, Pahl HL, Merfort I. The anti-inflammatory sesquiterpene lactone helenalin inhibits the transcription factor NF-kappaB by directly targeting p65. *J Biol Chem.* 1998; 273:33508–33516. [PubMed: 9837931]
63. Kawakami Y, Hartman SE, Kinoshita E, Suzuki H, Kitaura J, Yao L, Inagaki N, Franco A, Hata D, Maeda-Yamamoto M, Fukamachi H, Nagai H, Kawakami T. Terreic acid, a quinone epoxide inhibitor of Bruton's tyrosine kinase. *Proc Natl Acad Sci U S A.* 1999; 96:2227–2232. [PubMed: 10051623]
64. Iwamaru A, Szymanski S, Iwado E, Aoki H, Yokoyama T, Fokt I, Hess K, Conrad C, Madden T, Sawaya R, Kondo S, Priebe W, Kondo Y. A novel inhibitor of the STAT3 pathway induces apoptosis in malignant glioma cells both in vitro and in vivo. *Oncogene.* 2007; 26:2435–2444. [PubMed: 17043651]
65. Mylecharane EJ. 5-HT2 receptor antagonists and migraine therapy. *J Neurol.* 1991; 238(1):S45–52. [PubMed: 2045831]
66. Toullec D, Pianetti P, Coste H, Bellevergue P, Grand-Perret T, Ajakane M, Baudet V, Boissin P, Boursier E, Loriolle F, et al. The bisindolylmaleimide GF 109203X is a potent and selective inhibitor of protein kinase C. *J Biol Chem.* 1991; 266:15771–15781. [PubMed: 1874734]
67. Duan Z, Bradner JE, Greenberg E, Levine R, Foster R, Mahoney J, Seiden MV. SD-1029 inhibits signal transducer and activator of transcription 3 nuclear translocation. *Clin Cancer Res.* 2006; 12:6844–6852. [PubMed: 17121906]
68. Hiyama Y, Kuriyama K. Dissociation between antiinflammatory action of tilorone and its interferon inducing activity. *Agents Actions.* 1991; 33:229–232. [PubMed: 1719782]
69. Alonso-Gomez AL, Iuvone PM. Melatonin biosynthesis in cultured chick retinal photoreceptor cells: calcium and cyclic AMP protect serotonin N-acetyltransferase from inactivation in cycloheximide-treated cells. *J Neurochem.* 1995; 65:1054–1060. [PubMed: 7543927]

70. Blaskovich MA, Sun J, Cantor A, Turkson J, Jove R, Sehti SM. Discovery of JSI-124 (cucurbitacin D), a selective Janus kinase/signal transducer and activator of transcription 3 signaling pathway inhibitor with potent antitumor activity against human and murine cancer cells in mice. *Cancer Res.* 2003; 63:1270–1279. [PubMed: 12649187]
71. Schust J, Sperl B, Hollis A, Mayer TU, Berg T. Stattic: a small-molecule inhibitor of STAT3 activation and dimerization. *Chem Biol.* 2006; 13:1235–1242. [PubMed: 17114005]
72. Lipsky JJ, Shen ML, Naylor S. In vivo inhibition of aldehyde dehydrogenase by disulfiram. *Chem Biol Interact.* 2001; 130-132:93–102. [PubMed: 11306034]
73. Sharma SV, Agatsuma T, Nakano H. Targeting of the protein chaperone, HSP90, by the transformation suppressing agent, radicicol. *Oncogene.* 1998; 16:2639–2645. [PubMed: 9632140]
74. Kwon HJ, Yoshida M, Fukui Y, Horinouchi S, Beppu T. Potent and specific inhibition of p60v-src protein kinase both in vivo and in vitro by radicicol. *Cancer Res.* 1992; 52:6926–6930. [PubMed: 1458481]
75. Kreuter MH, Leake RE, Rinaldi F, Muller-Klieser W, Maidhof A, Muller WE, Schroder HC. Inhibition of intrinsic protein tyrosine kinase activity of EGF-receptor kinase complex from human breast cancer cells by the marine sponge metabolite (+)-aeropylsinin-1. *Comp Biochem Physiol B.* 1990; 97:151–158. [PubMed: 2253475]
76. Li YM, Mackintosh C, Casida JE. Protein phosphatase 2A and its [3H]cantharidin/[3H]endothall thioanhydride binding site. Inhibitor specificity of cantharidin and ATP analogues. *Biochem Pharmacol.* 1993; 46:1435–1443. [PubMed: 8240393]
77. Marmy-Conus N, Hannan KM, Pearson RB. Ro 31-6045, the inactive analogue of the protein kinase C inhibitor Ro 31-8220, blocks in vivo activation of p70(s6k)/p85(s6k): implications for the analysis of S6K signalling. *FEBS Lett.* 2002; 519:135–140. [PubMed: 12023032]

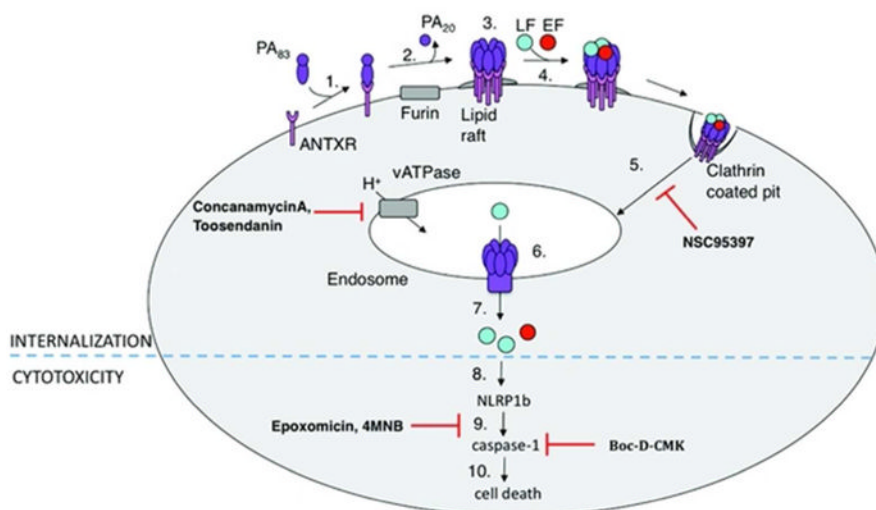


Figure 1. Cytoplasmic delivery of anthrax toxin 1. PA binds to one of two anthrax toxin receptors on the cell surface; 2. PA is processed by a host furin protease; 3. PA₆₃ remains bound to the receptor and oligomerizes into a heptamer or octamer; 4. binding of EF and/or LF; 5. clathrin-mediated endocytosis of the toxin-receptor complexes and trafficking to the endosome; 6. upon endosome acidification, PA undergoes a conformational change and forms a pore in the endosomal membrane; 7. translocation of EF and LF through the PA pore into the cytosol; 8. LF cleaves NLRP1b; 9. caspase-1 activation is dependent on proteasome activity; 10. caspase-1-dependent cell death.

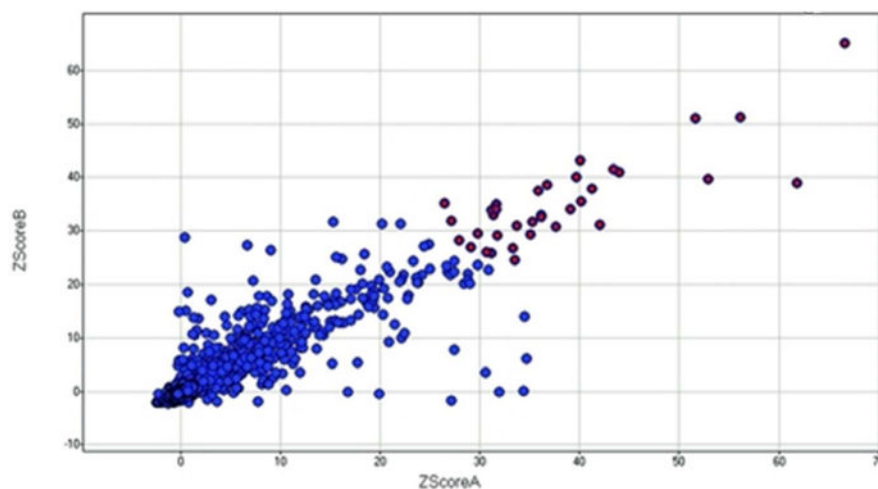


Figure 2. Small molecule screen: primary data from screening day 2. The plot shows the z score for replicates A and B for each compound screened. Compounds that were cherrypicked and retested are shown in red.

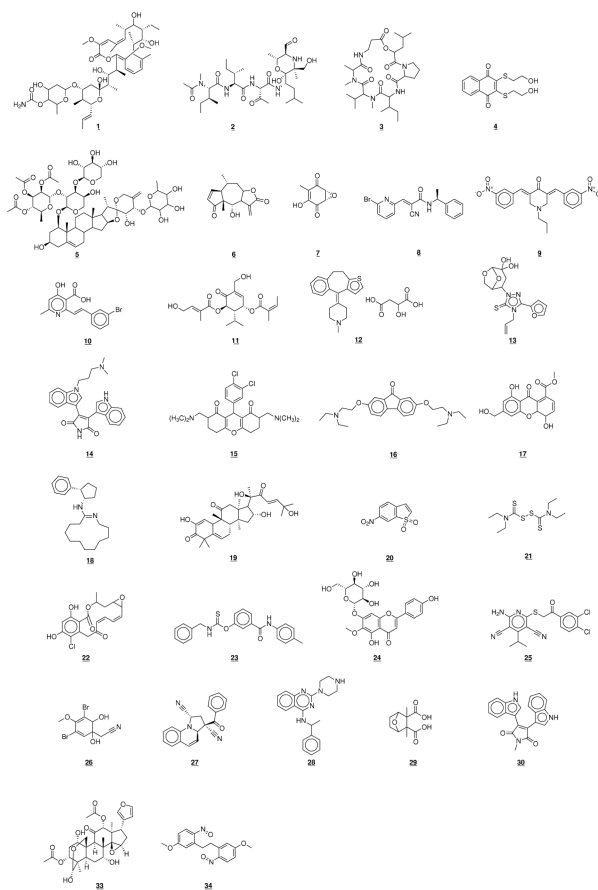


Figure 3. Structures of selected hits from the small molecule screen. Structures of compounds from Table 2.

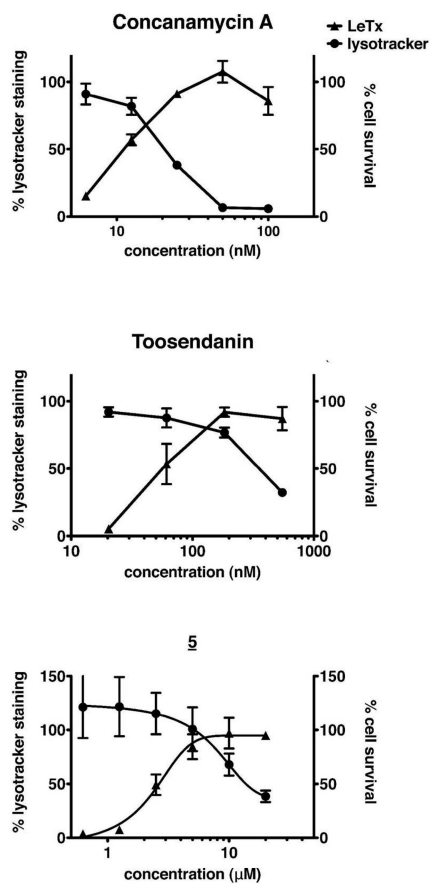


Figure 4. Internalization inhibitors of LT that inhibit endosome acidification Inhibition of lysotracker staining requires a higher concentration of compound than protection from LT.

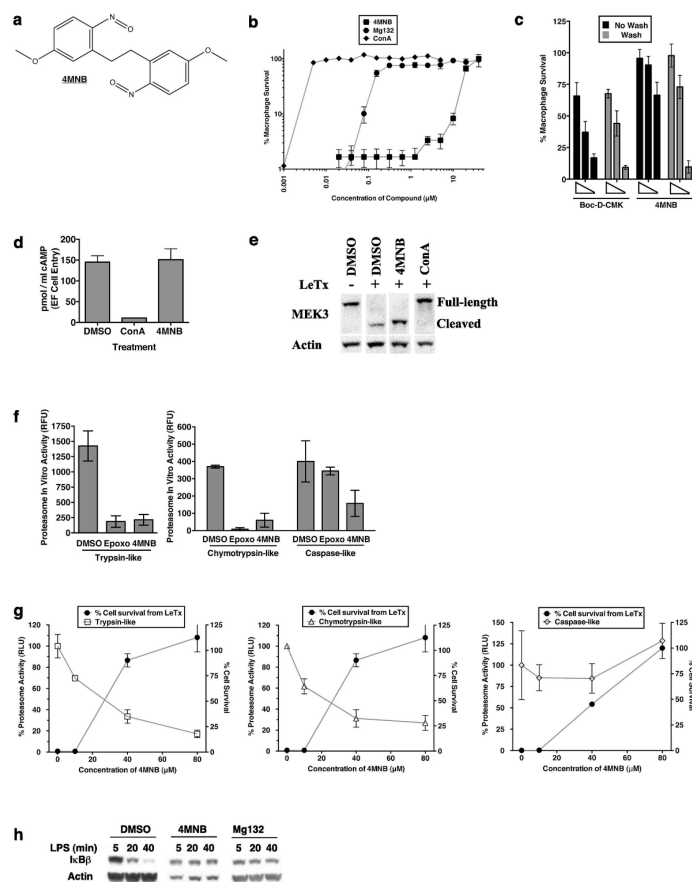


Figure 5. 4MNB protects against LT-induced cytotoxicity by inhibiting the proteasome a) Structure of 4MNB. b) J774 cells were treated with compound, followed by LT, and cell survival was measured. ConA is the internalization inhibitor concanamycin A and Mg132 is proteasome inhibitor that prevents LF-induced cytotoxicity. c) J774 cells were treated with compound (Boc-D-CMK 10, 5, 2.5 μM and 4MNB 80, 40, 20 μM), washed, exposed to LT, and cell survival measured. d) J774 cells were treated with compound (0.5 μM ConA and 40 μM 4MNB), exposed to ET, and cAMP levels were measured by ELISA. e) J774 cells were treated with compound (4MNB 40 μM and ConA 0.5 μM), exposed to LT, and lysates were probed for MEK3 cleavage. f) Lysates from J774 cells were treated with compound (Epoxo 10 μM and 4MNB 40 μM), incubated with substrates of the three proteasome proteases, and activity was determined by measuring fluorescence of cleaved substrates. g) J774 cells were treated with 4MNB and incubated with substrates of the proteasome or T. Proteasome activity was determined by measuring luminescence of leaved substrate and cell survival was measured. h) J774 cells were treated with compound (4MNB 80 μM and Mg132 20 μM), exposed to LPS (100 ng ml⁻¹), and lysate was collected and probed for evidence of I κ B β degradation.

Table 1

Compounds cherrypicked from small molecule screen.

Library	Screened	Cherrypicked
DOS	9570	23
Commerical	8580	31
Bioactives	6930	63
Natural Product extracts	3630	19
Purified Natural Products	2640	24
Total	31350	160

Table 2

Characterization of internalization inhibitors and selected control compounds from the small molecule screen. The minimum inhibitory concentration (MIC) required for 100% protection from LT and the concentration required for 50% protection (IC_{50}) are shown. All compounds designated as ET inhibitors inhibited at least 50% of cAMP induced by ET, while 4MNB and epoxomicin did not inhibit ET at all. Compounds that inhibited at least 50% of transferrin and dextran uptake were annotated as inhibitors of endocytosis. Protection of cells from TcdB-induced cell death ranged from 20-56%. Structures are shown in Figure 2. (n.d. = not done; *compound did not protect LFN-DTA or LT over 24 hour assay).

ID	Name	Function	LeTx MIC (μ M)	LeTx IC_{50} (μ M)	PA/LFN-DTA	EdTx	Transferrin/ dextran uptake	TcdB
1	Concanamycin A	Vacuolar ATPase inhibitor	0.001	0.0005	+	+	-	+
2	Epoxomicin	Proteasome inhibitor	0.125	0.04	*	-	-	-
3	Destruxin B (61)	Vacuolar ATPase inhibitor	0.625	0.156	+	+	n.d.	+
4	NSC 95397	Cdc25 protein phosphatase inhibitor or	1.25	0.625	toxic	+	+	+
5	ACon1_01348	Unknown	2.5	1.25	+	+	-	+
6	HelenaIn (62)	NF- κ B inhibitor	2.5	1.75	+	+	+	+
7	(-)-Terreic Acid (63)	BTK inhibitor (PH-domain)	10	4	toxic	+	+	-
8	WP1066 (64)	Stat3 inhibitor	5	2.5	n.d.	+	+	+
9	CBChromo1_0001 85	Unknown	5	1.25	toxic	+	+	+
10	CBChromo1_0001 86	Unknown	5	3.75	toxic	+	+	+
11	ACon1_00439	Unknown	5	3.5	toxic	+	+	+
12	Pizotifen malate (65)	Serotonin receptor antagonist	10	5	*	+	+	+
13	TimTecl_05928	Unkno wn	6.25	3.75	+	+	+	+
14	Bisindolylmaleimide I (66)	Protein kinase C inhibitor	7.5	1.875	+	+	+	+
15	SD-1029 (67)	JAK2 inhibitor	10	3.75	n.d.	+	+	+
16	Tilorone (68)	Induces interferon production	10	7.5	*	+	+	+
17	ACon1_01234	Unkno wn	10	5	+	+	+	+
18	MDL-12330A Hydrochloride (69)	Adenylate cyclase inhibitor or and calcium channel blocker	20	10	+	+	+	+
19	Cucurbitacin (70)	JAK/Stat3 inhibitor	20	10	toxic	+	+	+
20	Stat3ic (71)	Stat3 inhibitor	12.5	7.5	n.d.	+	n.d.	*
21	Disulfiram (72)	Aldehyde dehydrogenase inhibitor	20	7.5	*	+	+	+
22	Radicicol (73,74)	Hsp90 and Src kinase inhibitor	20	15	+	+	+	+
23	ChemDiv3_00721 3	Unknown	20	7.5	toxic	+	+	-

ID	Name	Function	LeTx MIC (μ M)	LeTx IC ₅₀ (μ M)	PA/LFn-DTA	EdTx	Transferrin/ dextran uptake	TcdB
24	ACon1_000166	Unkno wn	20	15	*	+	+	+
25	ChemDiv 0892-0507	Unkno wn	20	15	+	+	Inhibits dextran but not transferring uptake	+
26	Aeropylsinin-1 (75)	EGFR inhibitor	25	10	+	+	+	+
27	TimTec1_001156	Unknown	25	15	+	+	+	+
28	Neuro1_000172	Unknown	40	30	toxic	+	n.d.	+
29	Cantharidic Acid (76)	Protein Phosphatase2A inhibitor	>40	20	*	+	+	-
30	Bisindolylmaleimide V (77)	Negative control compo und for PKC inhibition studies	>40	20	+	+	n.d.	+
31	Natural product extract	Unknown	234 ng/mL	100 ng/mL	+	n.d.	-	-
32	Natural product extract	Unknown	29 ng/mL	10 ng/mL	+	n.d.	-	-
33	Toosendanin	Inhibitor of BoNT	0.183	0.06	+	n.d.	-	+
34	4MNB	Proteasome inhibitor	40	20	-	-	n.d.	+